

RESEARCH PAPER



The RNA binding protein Quaking represses host interferon response by downregulating MAVS

Kuo-Chieh Liao ^a, Vanessa Chuo^a, W. Samuel Fagg ^{b,c}, Shelton S. Bradrick^b, Julien Pompon ^{a,d*}, and Mariano A. Garcia-Blanco ^{a,b*}

^aProgramme in Emerging Infectious Diseases, Duke-NUS Medical School, Singapore; ^bDepartment of Biochemistry and Molecular Biology, The University of Texas Medical Branch, Galveston, TX, USA; ^cDepartment of Surgery, Transplant Division, The University of Texas Medical Branch, Galveston, TX, USA; ^dIRD, CNRS, Université de Montpellier, Montpellier, France

ABSTRACT

Quaking (QKI) is an RNA-binding protein (RBP) involved in multiple aspects of RNA metabolism and many biological processes. Despite a known immune function in regulating monocyte differentiation and inflammatory responses, the degree to which QKI regulates the host interferon (IFN) response remains poorly characterized. Here we show that QKI ablation enhances poly(I:C) and viral infection-induced IFN β transcription. Characterization of IFN-related signalling cascades reveals that QKI knockout results in higher levels of IRF3 phosphorylation. Interestingly, complementation with QKI-5 isoform alone is sufficient to rescue this phenotype and reduce IRF3 phosphorylation. Further analysis shows that MAVS, but not RIG-I or MDA5, is robustly upregulated in the absence of QKI, suggesting that QKI downregulates MAVS and thus represses the host IFN response. As expected, MAVS depletion reduces IFN β activation and knockout of MAVS in the QKI knockout cells completely abolishes IFN β induction. Consistently, ectopic expression of RIG-I activates stronger IFN β induction via MAVS-IRF3 pathway in the absence of QKI. Collectively, these findings demonstrate a novel role for QKI in negatively regulating host IFN response by reducing MAVS levels.

ARTICLE HISTORY

Received 26 June 2019
Revised 4 December 2019
Accepted 5 December 2019

KEYWORDS

QKI; IFN; IRF3; MAVS; viral infection

Introduction

The type I interferon (IFN) response is tightly regulated to mount efficient antiviral immunity while preventing autoimmunity [1]. IFN induction can be initiated upon recognition of pathogen associated molecular patterns (PAMPs) by several pattern recognition receptors (PRRs), including Toll like receptors (TLRs) [2] and retinoic acid-inducible gene I (RIG-I) like receptors (RLRs) [3]. Cytosolic detection of viral RNA by RIG-I or melanoma differentiation-associated gene 5 (MDA5), another member of the RLRs that has differential ligand specificity [4–6], changes the conformation of these receptors and enables their engagement with mitochondrial antiviral-signalling protein (MAVS) [7–10]. Subsequently, MAVS assembles into aggregates that trigger downstream signalling including activation and phosphorylation of interferon regulatory factor 3 (IRF3). Phosphorylated IRF3 translocates into the nucleus and, along with other transcription factors (e.g. ATF2 and cJun), drives the transcription of type I IFN β [11]. Synthesized IFN β proteins are then secreted and bind to the IFN receptor (IFNAR), which activates the Janus kinase (JAK)-signal transducer and activator of transcription protein (STAT) pathway and triggers the expression of hundreds of IFN-stimulated genes (ISGs) to establish an antiviral state in cells [12].

In addition to RLRs, which are responsible for sensing viral RNAs, several other RNA binding proteins (RBPs) play

important roles in modulating host IFN responses. These RBPs can act at different stages via distinct mechanisms. For example, during the early phase of infectious bursal disease virus infection, Staufen1 competes with MDA5 for viral RNA binding and attenuates MDA5-dependent IFN β induction [13]. In addition, zinc-finger RNA-binding protein (ZFR) can negatively regulate IFN β transcription. Specifically, ZFR promotes macroH2A1 expression via alternative splicing and consequently macroH2A1 binds and represses the IFN β promoter [14]. Hu antigen R (HuR) can bind and stabilize IFN β mRNA, thereby promoting the type I IFN response [15]. Moreover, multiple RBPs have been shown to regulate the expression and function of ISGs. These RBPs include G3BP1, G3BP2, and CAPRIN1 that promote the translation of ISG mRNAs and contribute to the establishment of an antiviral state [16]. DDX6 and Staufen1, on the contrary, can inhibit activation of ISGs [17,18]. Additionally, there is an overrepresentation of RBPs among ISGs [19].

Quaking (QKI) is a member of the signal transduction and activator of RNA (STAR) family of hnRNP K homology (KH)-type RBPs. Three main isoforms of QKI (QKI-5, QKI-6, and QKI-7) are produced from a single gene by alternative splicing [20,21]. A major difference among these isoforms is their sub-cellular localization: QKI-5 is localized to the nucleus [22]; QKI-6 is distributed throughout the cell while QKI-7 is mainly cytosolic [23]. QKI proteins are involved in multiple aspects of RNA

CONTACT Kuo-Chieh Liao  kc.liao@duke-nus.edu.sg; Mariano A. Garcia-Blanco  maragarc@utmb.edu  Programme in Emerging Infectious Diseases, Duke-NUS Medical School, Singapore

*These authors contributed equally to this work.

 Supplemental data for this article can be accessed here.

© 2019 Informa UK Limited, trading as Taylor & Francis Group

metabolism [24], such as alternative splicing [25–30], mRNA stability [31,32] and microRNA biogenesis [33–35]. These processes are regulated by QKI binding to an RNA element, known as the QKI response element (QRE) [36]. Dysregulation of QKI-mediated biological activities has been implicated in several human diseases, such as atherosclerosis [37] and cancer [38–41]. Recently, QKI has been shown to play versatile roles in regulating viral infection [42–44]. QKI was shown to facilitate the expression of viral proteins and the production of infectious viral particles in herpes virus infected cells [42]. A pro-viral role for QKI was observed with Zika virus infection [43]. Intriguingly, QKI inhibits viral replication of a clinical isolate of DENV4 by binding to the QRE in its 3' UTR [44]. Nonetheless, it is unclear how or if QKI regulates the IFN response.

Here we determine the function of QKI in the IFN response by using CRISPR-Cas9 technology to generate QKI knockout (QKO) cells. In the absence of QKI, transfection of poly(I:C), a double-stranded RNA (dsRNA) analogue, results in elevated IFN β transcription, suggesting that QKI is a negative regulator of IFN induction. Investigation of poly(I:C)-induced signalling cascades indicates increased phosphorylation of IRF3 in the QKO cells. Interestingly, complementation with the QKI-5 isoform alone rescues this phenotype and reduces IRF3 phosphorylation, indicating that this isoform is sufficient for the negative regulation of IRF3 phosphorylation. Additionally, we observe upregulation of MAVS at the protein level in the QKO cells, suggesting a potential pathway through which QKI represses host IFN response. As expected, subsequent depletion of MAVS in the QKO cells leads to reduced IFN β transcription. Altogether, this study demonstrates a novel role of QKI in negatively regulating host IFN response by reducing MAVS levels.

Results

QKI downregulates IFN induction

To investigate the role of QKI in host IFN response, we first generated QKI KO (QKO) HuH7 cells using CRISPR-Cas9 technology. QKI guide RNA (gRNA) was designed to target a common exon in all QKI isoforms and thus this genetic manipulation resulted in the loss of expression of QKI-5, QKI-6, and QKI-7. In Fig. 1A, QKO#3 and QKO#6 do not express QKI proteins as shown by immunoblotting analysis. Additionally, genotyping analysis shows that genetic mutations in these QKO cells cause a frameshift in the QKI open reading frame (ORF) (Table S1 and S2), which should lead to the production of truncated QKI proteins and/or nonsense-mediated decay (NMD). Notably, genotyping analysis indicates that QKO#3 and QKO#6 are genetically independent. Each of them harbours distinct insertion or deletion mutations. This genetic difference can account for some phenotypic variability in these two clonal QKO cells. To test the effect of QKI on IFN β transcription, we treated parental HuH7 or QKI KO HuH7 cells with poly(I:C) in the presence or absence of transfection reagent. Four hours later, total cellular RNA was isolated and analysed for IFN β mRNA abundance by RT-qPCR. Relative levels of IFN β mRNA were normalized to the geometric mean of two reference genes, *SDHA* and *HPRT1*, and are expressed relative to the untreated control. Transfection of poly(I:C) into WT cells induced robust IFN β transcription in a dose-dependent manner

(T-0.5 μ g and T-2 μ g) whereas direct treatment of 5 μ g/mL poly(I:C) failed to activate IFN β transcription (Fig. 1B). This is because HuH7 cells lack sufficient expression of TLR3, which is important for responding to extracellular poly(I:C) [45]. Transfected poly(I:C), on the contrary, can be recognized by RIG-I and/or MDA5 to activate IFN β transcription in cells [6,46]. Interestingly, we observed about 2-fold higher induction of IFN β mRNA levels by poly(I:C) in the two independent QKO cells (Fig. 1B,C). To determine if this increase was at the transcriptional level, we co-transfected a IFN β reporter plasmid along with a reference luciferase plasmid into WT and the QKO#3 cells and measured relative luciferase activity in the absence or presence of poly(I:C) transfection. This IFN β reporter plasmid contains two copies of human IFN β promoter sequences upstream to a firefly luciferase, which allows us to assess the IFN β promoter activity in cells. In addition, co-transfection of the reference *Renilla* luciferase plasmid was used as a control for transfection efficiency. We found that the QKO#3 cells exhibit a moderately higher level of basal IFN β reporter activity as compared with WT cells in the absence of poly(I:C) (Fig. 1D). Upon poly(I:C) stimulation, the QKO#3 cells showed a ~200 fold induction in relative luciferase activity compared to only ~50 fold induction in poly(I:C)-transfected WT cells, further supporting the notion that QKI negatively regulates IFN β transcription. Furthermore, Sendai virus (SeV) infection triggered a ~2-fold higher IFN β reporter activity in QKO#3 cells relative to WT cells (Fig. 1E and Fig. S1). These results suggest that QKI represses IFN β transcription following viral infection or intracellular dsRNA recognition.

To test whether biologically active IFN proteins are secreted from the QKO cells, we transfected poly(I:C) into WT and QKO#3 cells and collected the conditioned media 4h post-transfection. These conditioned media were subsequently applied to WT HuH7 cells and the protein levels of two ISG family members (PKR and IFITM2) were measured by Western blotting. Consistent with enhanced IFN β activation in the QKO cells, conditioned media from poly(I:C)-transfected QKO#3 induced ~18% higher PKR and ~28% higher IFITM2 protein levels than that from poly(I:C)-transfected WT cells (Fig. 1F), suggesting that higher amounts of ISG inducing proteins, likely IFNs, are secreted from the QKO cells.

Next, to test if QKI affects ISG expression, we treated WT and the QKO cells with IFN β proteins and analysed expression of selected ISG proteins. IFN β treatment caused a 2-fold increase in PKR expression in WT, the QKO#3 and the QKO#6 cells (Fig. S2). No difference in PKR expression was detected between WT and the QKO cells. In addition, ISG15 induction level was similar across all these cells upon IFN β treatment, indicating that QKI is not involved in regulating PKR and ISG15 expression in IFN-treated cells. Taken together, these data suggest that QKI inhibits the IFN response by downregulating the transcriptional induction of IFN β .

De-repression of IRF3 activation in the absence of QKI

Since we observed higher transcription of IFN β reporter in the absence of QKI (Fig. 1D), we investigated IRF3 and other transcription factors (e.g. ATF2 and cJun) that are activated and recruited to the IFN β promoter for optimal induction of IFN β expression [11,47]. We first probed for phosphorylated IRF3

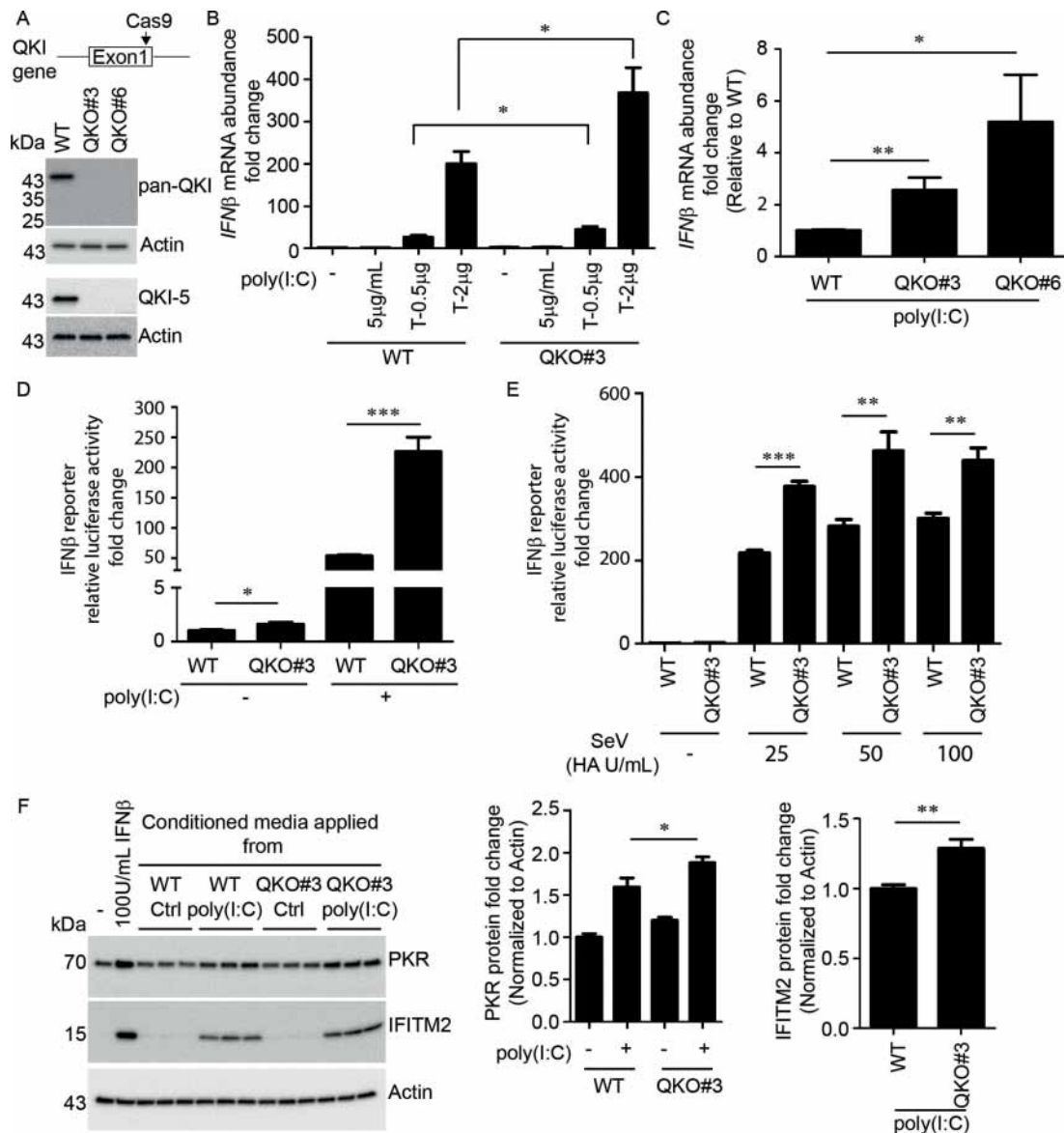


Figure 1. QKI negatively regulates host IFN response.

(A) Representative immunoblotting results showing KO of QKI expression in the QKO#3 and QKO#6 cells. (B) HuH7 WT and the QKO#3 cells were left untreated, directly incubated with poly(I:C) (5 μg/mL), or transfected with poly(I:C) using RNAiMAX (T-0.5 μg or T-2 μg) for 4h. Levels of *IFNβ* RNA abundance were subsequently measured by RT-qPCR. (C) Accumulation of *IFNβ* RNA in HuH7 WT and the two QKO cells was assessed 4h post poly(I:C) transfection (2 μg) by RT-qPCR. The data were reported relative to the WT samples. (D) *IFNβ* F Luc reporter plasmids were co-transfected with R Luc plasmids into HuH7 WT and the QKO#3 cells. Approximately 24h after transfection, cells were transfected with 2 μg poly(I:C) for 8h and luciferase activity was measured using the dual luciferase assay. F Luc signals were normalized first to R Luc signals, and relative luciferase activity fold change was reported relative to untransfected WT samples. (E) HuH7 WT and the QKO#3 cells were co-transfected with *IFNβ* F Luc plasmids and R Luc plasmids. On the following day, cells were infected with increasing doses of Sendai virus (SeV). At 16h post infection, cell lysates were harvested and analysed using the dual luciferase assay. F Luc signals were normalized first to R Luc signals, and relative luciferase activity fold change was reported relative to uninfected WT samples. (F) Conditioned media from poly(I:C)-transfected (1 μg) HuH7 WT and the QKO#3 cells were applied to HuH7 WT cells. After 18h incubation, cell lysates were harvested and probed for indicated proteins by immunoblotting. Representative blots from two independent experiments are shown. Densitometry analysis of Western Blot (WB) data was performed to determine relative levels of PKR and IFITM2 proteins. Data are mean ± S.E.M from at least two independent experiments and each experiment had three wells that were treated independently (replicates ≥ 6). Statistical significance was determined using a two-tailed *t* test: *, *p* < 0.05; **, *p* < 0.01; ***, *p* < 0.001.

(pIRF3) and total IRF3 proteins in WT and the QKO cells at 1.5h, 2.5h, 4.5h and 6h after poly(I:C) transfection. Interestingly, we observed higher levels of phosphorylated IRF3 in both QKO#3 and QKO#6 cells at 4.5h and 6h after poly(I:C) transfection (Fig. 2A), despite a slight difference in IRF3 phosphorylation kinetics between these two QKO clonal cells. Total levels of IRF3 remained relatively unaltered by QKI KO (Fig. 2A). Next, we probed for phosphorylated ATF2 (pATF2) and phosphorylated cJun (pcJun) in WT and the two QKO cells. As expected, poly(I:C) transfection resulted in the phosphorylation of ATF2 and

cJun across all cell lines (Fig. S3); however, the phosphorylation levels of these two transcription factors were unaltered by QKI KO (Fig. S3). These results suggest that QKI represses poly(I:C)-induced phosphorylation of IRF3 but not of ATF2 and cJun.

IRF3 activates gene expression in targets other than *IFNβ*; transcriptional profiling revealed that two ISGs, IFIT1 and IFIT2, are also activated by IRF3 [48]. In addition, the expression of *IFNλ1*, a type III interferon, is activated by IRF3 [49,50]. Since higher phosphorylated IRF3 levels were detected in the absence of QKI, we hypothesized that other IRF3-dependent genes should be

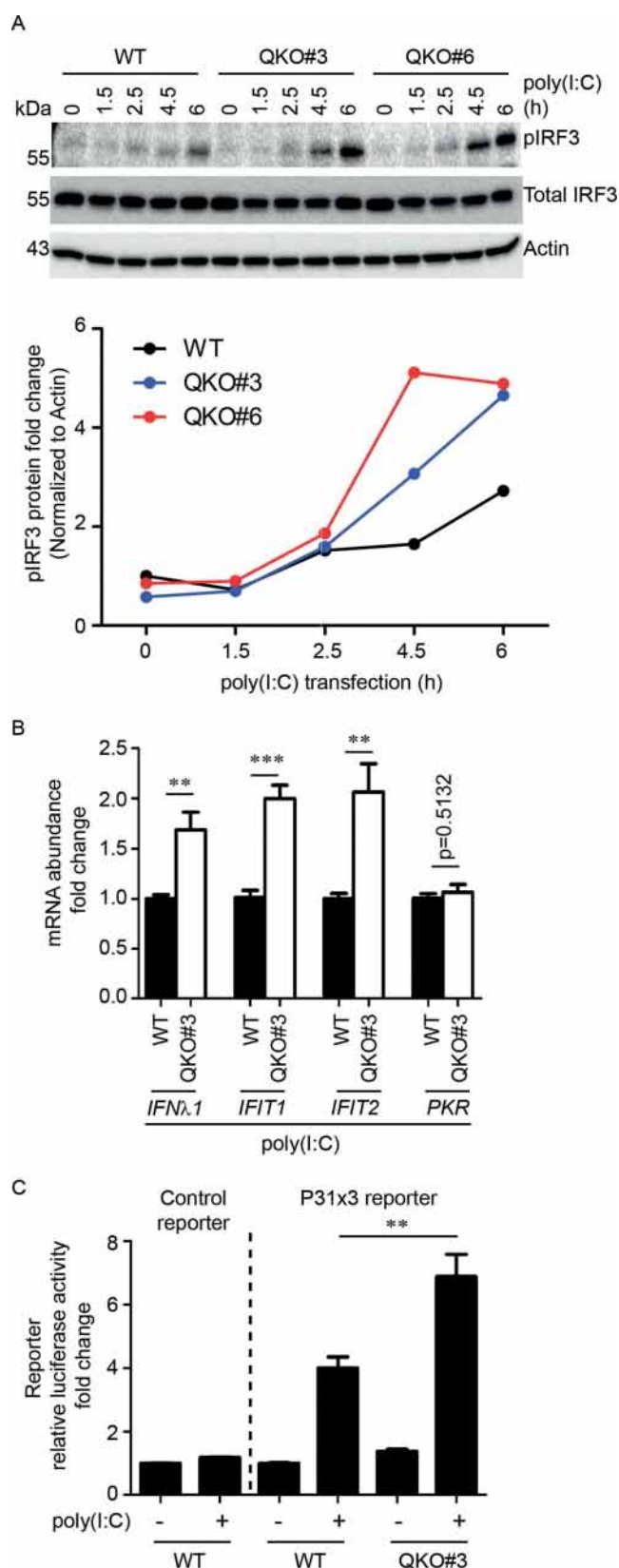


Figure 2. Increased IRF3 phosphorylation and upregulation of IRF3-dependent genes in the absence of QKI upon poly(I:C) transfection.

(A) Representative immunoblots from 3 independent experiments indicating phosphorylated IRF3 (pIRF3) and total IRF3 in HuH7 WT and the two QKO cells at different time points after poly(I:C) transfection (2 μ g). Densitometry analysis of WB data was performed to determine relative levels of pIRF3 proteins. The data were normalized actin and the values were reported relative to the untransfected WT samples. (B) Total RNA was isolated from HuH7 WT and the QKO#3 cells at 4h post-poly(I:C) transfection (2 μ g). RNA abundance of indicated genes was measured using RT-qPCR. (C) HuH7 WT and the QKO#3 cells were transfected with control empty reporter plasmids or P31x3 reporter plasmids containing three copies of the IRF3-responsive element in the promoter region. On the following day, cells were transfected with 2 μ g poly(I:C) for 8h and cell lysates were harvested and analysed by the dual luciferase assay. R Luc signals were normalized first to F Luc signals, and relative luciferase activity fold change was reported relative to untransfected WT samples. Data are mean \pm S.E.M from two independent experiments and each experiment had three wells that were treated independently (replicates = 6). Statistical significance was determined using a two-tailed *t* test: **, *p* < 0.01; ***, *p* < 0.001.

upregulated in the QKO cells. Indeed, RT-qPCR analysis indicated that *IFN λ 1*, *IFIT1*, and *IFIT2* mRNA abundance was higher in the QKO#3 cells as compared with WT cells (Fig. 2B). No difference in *PKR* mRNA levels, which is not regulated directly by IRF3, was observed between WT and the QKO#3 cells. To further test if IRF3-dependent genes are repressed by QKI, we constructed a psiCHECK2 reporter plasmid that has three copies of the IRF3 response element (P31x3) in the promoter region [51]. As expected, when cells were transfected with control empty reporter plasmids that do not contain IRF3 response element, no induction of reporter activity was detected upon poly(I:C) transfection (Fig. 2C). Transfection of P31x3 reporter plasmids, instead, resulted in a ~4-fold increase of relative luciferase activity in WT cells upon poly(I:C) stimulation, and ~7-fold in the QKO#3 cells (Fig. 2C). Altogether, these data suggest that QKI represses IRF3-phosphorylation.

QKI-5 downregulates IRF3 phosphorylation

There are three major isoforms of QKI, all of which have overlapping but distinct biological functions [23,24]. To test if QKI-5 alone can repress IRF3 phosphorylation, we generated a QKO#3 polyclonal stable cell line expressing N-terminal FLAG-QKI5 (Q5B) (Fig. 3A). WT, QKO#3, and Q5B cells were transfected with poly(I:C) and IRF3 phosphorylation was assessed by immunoblotting. Consistent with previous results (Fig. 2A), higher levels of phosphorylated IRF3 were detected in the QKO#3 cells upon poly(I:C) transfection (Fig. 3B). Strikingly, expression of QKI-5 alone reversed the phenotype seen in the QKO#3 cells and showed lower levels of IRF3 phosphorylation (Fig. 3B). To further determine if the expression level of QKI-5 has an impact on IRF3 phosphorylation, we performed limiting serial dilution to isolate clonal cells that express various levels of QKI-5. Three cell lines were selected: one with low QKI-5 level (Q5B2), one with intermediate QKI-5 level (Q5B4), and one with high QKI-5 level (Q5B6) (Fig. S4A). Repression of IRF3 phosphorylation was observed in Q5B4 cells but not in Q5B2 and Q5B6 cells (Fig. S4B, S4C, and S4D), which is consistent with the notion that an optimal 'setting' of QKI levels is required for cell type-specific homeostatic gene expression [26]. These results suggest that an optimal expression level of QKI-5 is critical for the negative regulation of IRF3 phosphorylation, and the QKI-5 isoform is sufficient for repression of IRF3 phosphorylation.

QKI negatively regulates MAVS level

To further investigate the mechanism by which QKI KO increases IRF3 phosphorylation, we measured key regulators upstream of IRF3 in the type I IFN induction pathway. Firstly, we probed for RIG-I in WT cells and the two QKO cells. Although a 20% increase of RIG-I protein level was observed in the QKO#3 cells relative to WT cells, this RIG-I increase was not observed in the QKO#6 cells (Fig. 4A). In addition, changes in MDA5 protein levels in the two independent QKO cells were inconsistent (Fig S5A and S5B). These results suggest that elevated IRF3 phosphorylation is independent of RIG-I and MDA5 protein levels. Next, we measured MAVS protein levels in these cells and found it was increased by ~50% in the two

QKO cells as compared with WT cells (Fig. 4A). Furthermore, the elevated MAVS levels persisted following poly(I:C) treatment but were not elevated significantly above no treatment levels (Fig. 4B). To further confirm that QKI downregulates MAVS expression, we knocked out QKI in A549 cells (Fig. S6A and Table S1 and S2) and measured MAVS protein level by immunoblotting. Consistent with the observation in HuH7 cells, MAVS was upregulated in the absence of QKI in A549 cells (Fig. S6B). Intriguingly, this increase in abundance was only observed at the protein level. Indeed, MAVS mRNA abundance was lower in QKO#3 and QKO#6 cells, albeit not statistically significant in the latter (Fig. 4C). Taken together, these results indicate that QKI KO causes an increase of MAVS protein expression, and thus QKI is a negative regulator of MAVS abundance.

QKI-5 associates with MAVS RNA

To investigate the mechanism by which QKI downregulates MAVS, we wanted to test if QKI-5 binds to MAVS RNA since QKI-5 alone is sufficient to repress IRF3 phosphorylation. To address this question, we performed RNA immunoprecipitation (RIP) followed by RT-qPCR analysis. We used HEK293 cells expressing N-terminus FLAG tagged QKI-5 isoform under the control of a tetracycline-inducible promoter. These cells were first treated with tetracycline for 18h to induce FLAG-QKI-5 expression. Then cell lysates were harvested and immunoprecipitated using a mouse IgG control antibody or a mouse FLAG antibody. Total RNA was purified from the immunoprecipitated material for RT-qPCR analysis. Data are presented as the degree of enrichment of the indicated RNAs present in the FLAG IP sample relative to the isotype control. In Fig. 5A, only FLAG antibody efficiently immunoprecipitated FLAG-QKI-5 from lysates. RT-qPCR results indicate that there was a ~10 to 15-fold enrichment of MAVS RNA in FLAG IP samples, suggesting that QKI-5 interacts with MAVS RNA (Fig. 5B). As expected, CTNNB1 and hnRNPA1 RNAs, which were previously shown to bind QKI-5 [44], were enriched in FLAG IP samples. As a negative control, SF3B1 RNA was not enriched in FLAG IP complexes (Fig. 5B). Taken together, the data suggest that QKI-5 directly represses MAVS expression through its interaction with MAVS RNA.

A pivotal role for MAVS in type I interferon induction in the QKO cells

MAVS is an essential component for type I interferon induction and its expression level is intricately regulated [8,52,53]. To test if MAVS upregulation promotes enhanced IFN β induction in the QKO cells, we used CRISPR-Cas9 gene editing to deplete MAVS in the QKO cells and examined the induction of an IFN β reporter plasmid in these cells. We observed ~60% reduction of MAVS expression in both WT_sgMAVS and QKO#3_sgMAVS cells (Fig. 6A). In accordance with the literature, reduction of MAVS protein resulted in the decrease of IFN β reporter relative luciferase activity (Fig. 6B). Although the QKO#3_sgMAVS cells have less MAVS protein than WT cells at the total population level (Fig. 6A), IFN β was induced at similar levels (Fig. 6B). If residual

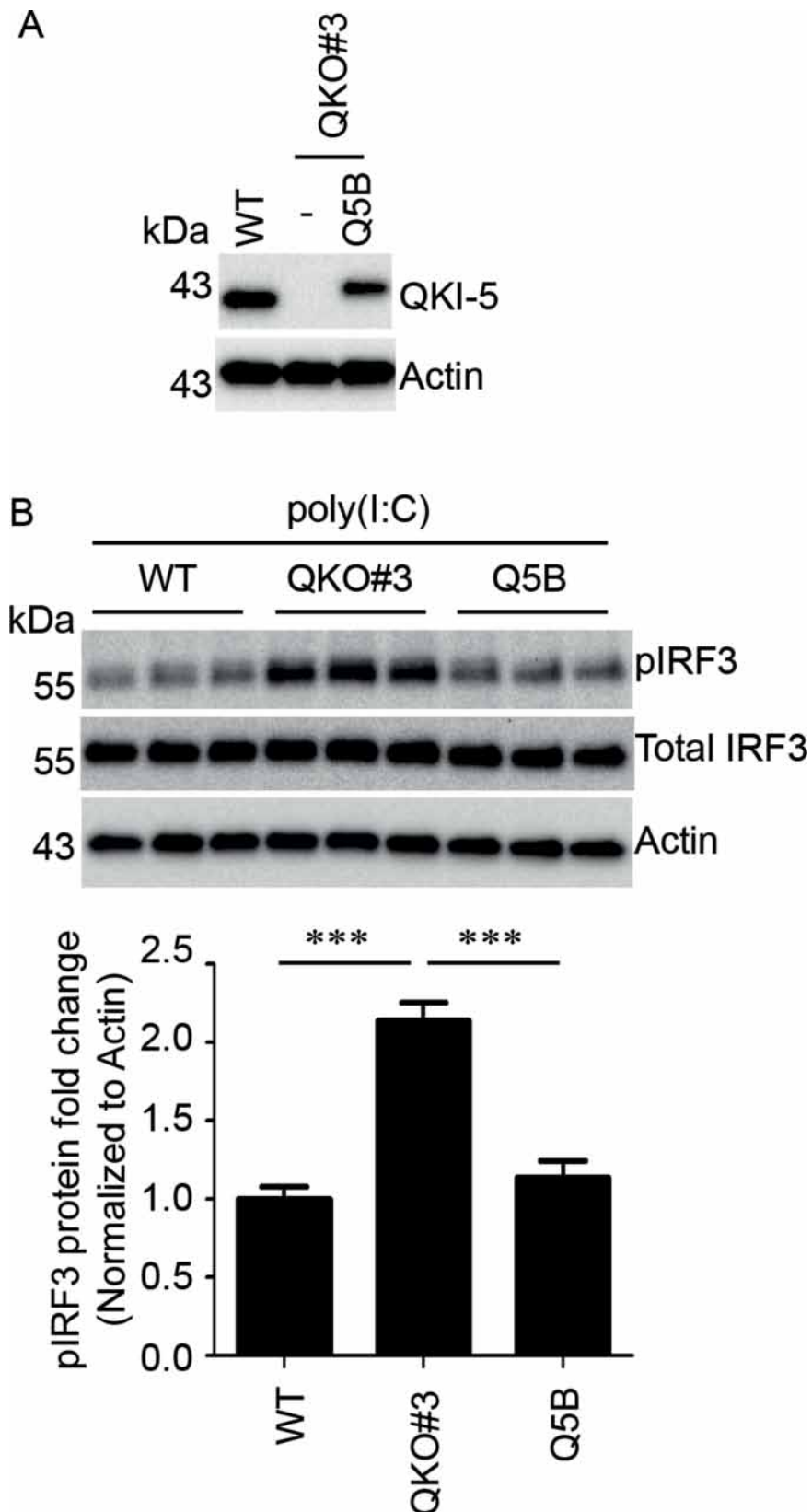


Figure 3. QKI-5 isoform is sufficient for repressing IRF3 phosphorylation.

(A) Representative immunoblotting results showing the expression level of QKI-5 in the complemented Q5B cells from at least two independent experiments. (B) Cells were transfected with 2 μ g poly(I:C) for 4h. After poly(I:C) transfection, HuH7 WT, the QKO#3 and the Q5B cells were lysed and lysates were probed for phosphorylated IRF3, total IRF3, and actin. Representative blots from two independent experiments are shown. Densitometry analysis of WB data was performed to determine relative levels of pIRF3 proteins. Data are mean \pm S.E.M from two independent experiments and each experiment had three wells that were treated independently (replicates = 6). Statistical significance was determined using a two-tailed *t* test: ***, *p* < 0.001.

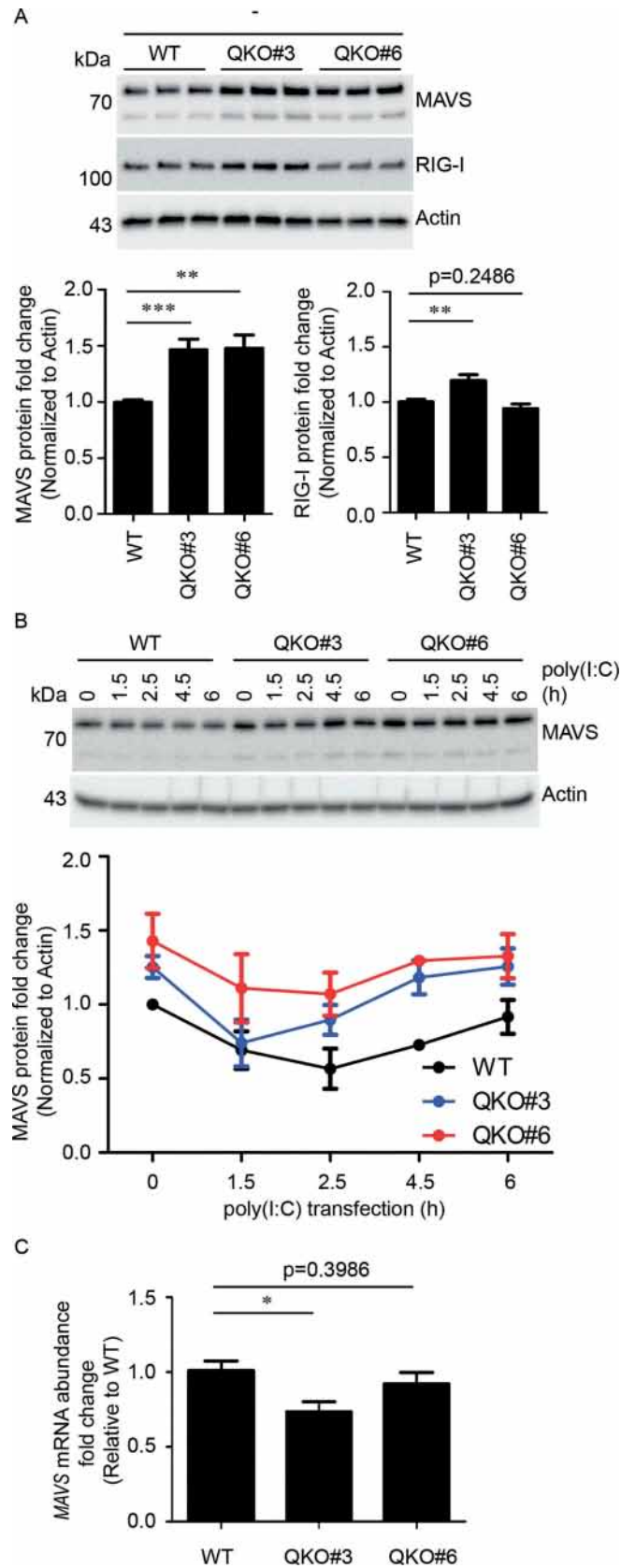


Figure 4. QKI reduces MAVS protein level.

(A)(B) HuH7 WT and the two QKO cells were left untreated or transfected with 2µg poly(I:C). Cells were then harvested at various time points and lysates were probed for indicated proteins using immunoblotting. Representative blots from two independent experiments are shown. Densitometry analysis of WB data was performed to determine relative levels of RIG-I and MAVS proteins. The data were normalized to actin and the values were reported relative to the untransfected WT samples. (C) MAVS RNA abundance in untreated HuH7 WT and the two QKO cells were assessed by RT-qPCR. Data were reported relative to the WT samples. Data are mean ± S.E.M from two independent experiments and each experiment had three wells that were treated independently (replicates = 6). Statistical significance was determined using a two-tailed *t* test: *, *p* < 0.05; **, *p* < 0.01; ***, *p* < 0.001.

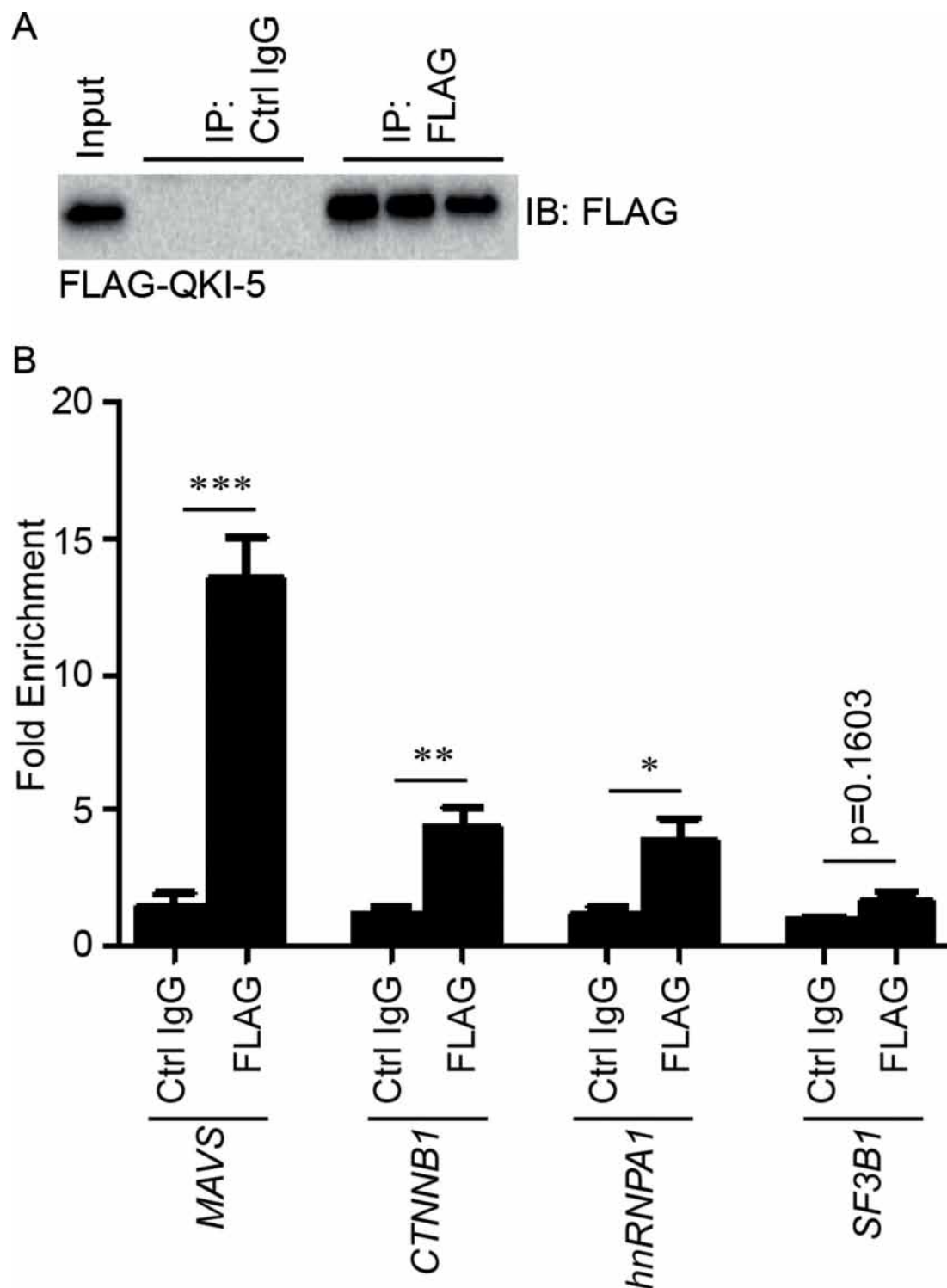


Figure 5. QKI-5 interacts with MAVS RNA.

(A) Immunoprecipitated FLAG-tagged QKI-5 was detected via immunoblotting in input samples and immunoprecipitated materials by using antibody against FLAG tag. (B) Total RNA was isolated from immunoprecipitated materials and RNA abundance of indicated genes was analysed by RT-qPCR. Data are mean \pm S.E.M from two independent experiments and each experiment had three wells that were treated independently (replicates = 6). Statistical significance was determined using a two-tailed *t* test: *, $p < 0.05$; **, $p < 0.01$; ***, $p < 0.001$.

MAVS expression within a mixed population of QKI-null cells is responsible for this reporter activity, then clonal selection of true MAVS-null cells should result in loss of this effect. To test this hypothesis, we performed limiting serial dilution of the QKO#3_sgMAVS cells and isolated two genetically independent

QKO cells that do not express MAVS, QKO#3_MKO#1 and QKO#3_MKO#10 (Fig. 6C and Table S1). The IFN competence of these two cells was subsequently evaluated by IFN β reporter assay. Indeed, loss of MAVS in the QKO#3_MKO#1 and QKO#3_MKO#10 cells abolished poly(I:C)-induced IFN β

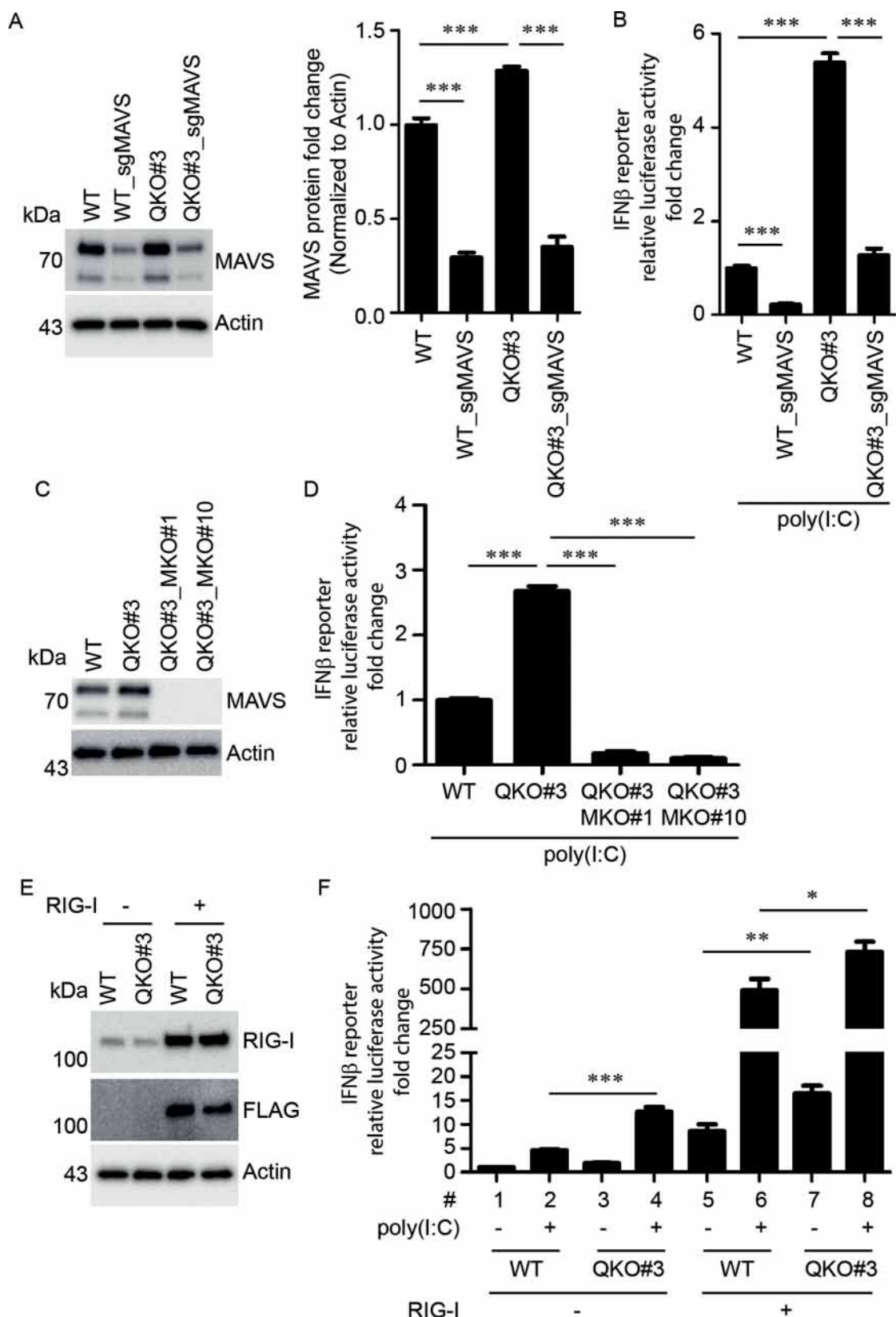


Figure 6. An essential role for MAVS in regulating IFN β transcription.

(A)(C) Representative immunoblots indicating the expression level of MAVS in various cells from at least two independent experiments. Densitometry analysis of WB data was performed to determine relative levels of MAVS proteins. (B)(D) Cells were transfected with IFN β F Luc plasmids and R Luc plasmids. On the following day, after transfection with 2 μ g poly(I:C) for 8h, cells were harvested and lysates were analysed using the dual luciferase assay. F Luc signals were normalized first to R Luc signals, and relative luciferase activity fold change was reported relative to WT samples. (E)(F) HuH7 WT and the QKO#3 cells were co-transfected with IFN β F Luc plasmids, R Luc plasmids, and empty vectors or plasmids encoding FLAG-tagged RIG-I. Approximately 24h after transfection, cells were left untreated or transfected with 2 μ g poly(I:C) for 8h. Subsequently, cell lysates were harvested and analysed by immunoblotting and the dual luciferase assay. F Luc signals were normalized first to R Luc signals, and relative luciferase activity fold change was reported relative to untransfected WT samples. Data are mean \pm S.E.M from at least two independent experiments and each experiment had three wells that were treated independently (replicates \geq 6). Statistical significance was determined using a two-tailed *t* test: *, *p* < 0.05; **, *p* < 0.01; ***, *p* < 0.001.

transcription (Fig. 6D). Thus, MAVS is required for robust IFN induction in the presence and absence of QKI.

Upon ligand RNA recognition, RIG-I interacts with MAVS and triggers signalling cascades that lead to IFN β activation [54], and ectopic expression of RIG-I alone is sufficient to activate IFN β transcription [8,55]. To test if ectopic expression of RIG-I induces stronger IFN β activation in the absence of QKI, IFN β reporter plasmids and RIG-I plasmids were co-transfected into WT and the QKO#3 cells, and dual luciferase assays were conducted in the absence or presence of poly(I:C) transfection. Ectopic RIG-I expression (Fig. 6E) was sufficient to activate IFN β transcription without poly(I:C) transfection (Fig. 6F). This activation was enhanced by approximately 2-fold in the QKO#3 cells compared to WT cells (Fig. 6F, compare bar #5 and #7). In addition, with combined ectopic RIG-I expression and poly(I:C) transfection, we observed a ~ 50% higher IFN β reporter activity in the QKO#3 cells than that in WT cells. Taken together, these results suggest that QKI represses IFN β induction triggered through the RIG-I-MAVS axis (Fig. 7).

Discussion

Here we show that QKI negatively regulates IFN induction upon poly(I:C) transfection and SeV infection. In fact, accumulating evidence suggests that RBPs regulate not only type I IFN, but also type II and type III IFNs. TTP has been shown to mediate IFN γ mRNA decay [56], and KSRP depletion enhances IFN λ 3 mRNA stability [57]. These reports further underscore the importance of RBPs in regulating host IFN response. Recently, Witteveldt et al. demonstrated a feedback loop regulation of Microprocessor activity during the activation of the IFN response [58]. Activation of IFN expression alters the binding of the Microprocessor complex to a subset of pri-miRNAs, which reduces its processing rate and thus leads to decreased levels of mature miRNAs. Interestingly, rescue of Microprocessor function by ectopic expression of DGCR8 and Drosha dampens IFN β induction [58]. It is known that QKI regulates miRNA biogenesis via, at least in part, interaction with DGCR8 and Drosha [35]. This study adds QKI to a growing group of RBPs in IFN regulation.

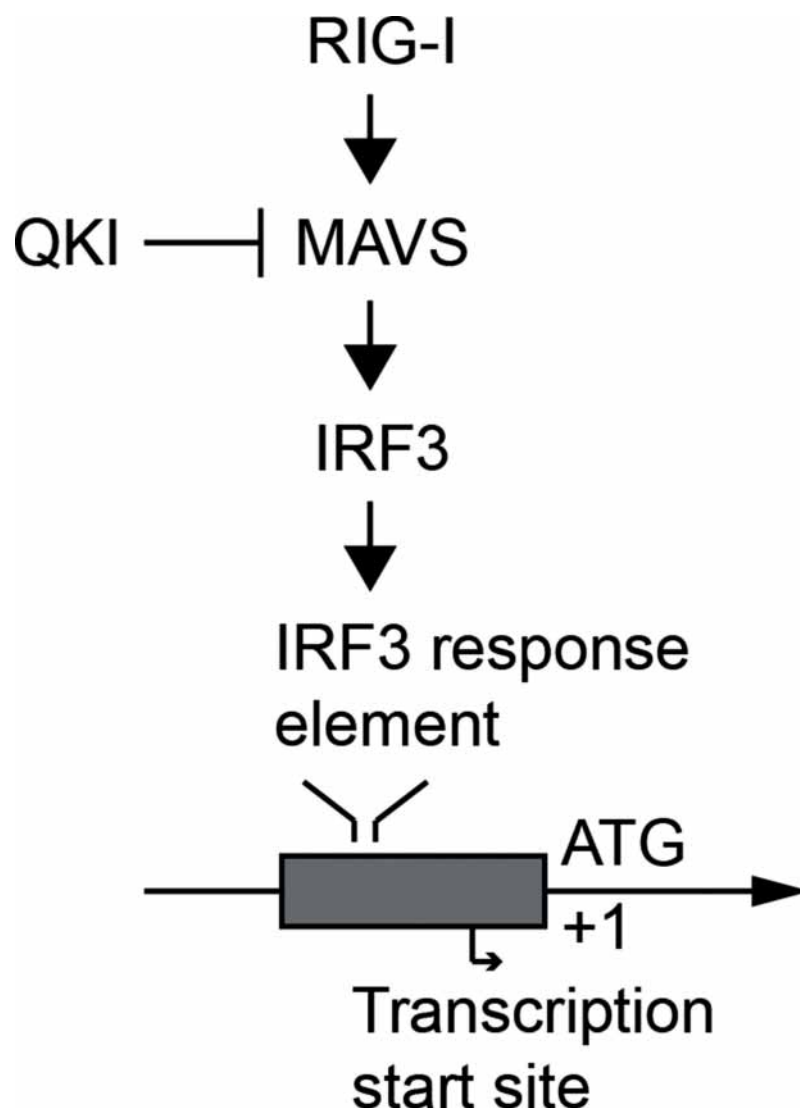


Figure 7. A schematic model demonstrating that QKI represses IRF3 dependent gene expression by negatively modulating MAVS levels.

MAVS is an essential adaptor to activate IFN response upon viral RNA recognition by RIG-I or MDA5 [59]. We show that QKI KO results in an upregulation of MAVS protein level in both HuH7 and A549 cells (Fig. 4A, 4B and S6B). Similar upregulation was not observed for RIG-I and MDA5, suggesting that this QKI-mediated upregulation of protein level is specific to MAVS. Consistent with our findings, a recent report demonstrated that upregulation of MAVS results in spontaneous activation of antiviral signalling cascade and higher basal IFN β expression in cardiac myocytes [60]. In fact, MAVS expression needs to be tightly regulated to prevent aberrant innate immune activation. This regulation can be achieved by post-translational modification [53]. Additionally, regulation of MAVS levels can be achieved at the post-transcriptional level through targeting of MAVS mRNA 3' UTR by microRNAs [52,61,62]. Our RT-qPCR analysis shows that MAVS mRNA abundance is not significantly altered in WT and the QKO cells, suggesting that QKI may not affect MAVS at the transcriptional level. Instead, the moderate yet robust increase (almost 50%) of MAVS protein level by QKI KO may be a result of QKI-mediated microRNA biogenesis, since effects that are 2-fold or lower are typically observed in microRNA-regulated events [63]. That said, our RIP results suggest that it is more likely that QKI regulates MAVS mRNA translation efficiency by direct QKI-MAVS RNA interactions.

Upon viral infection, multiple transcription factors induce type I IFN induction. We first examined the phosphorylation status of IRF3 in poly(I:C) transfected cells and found that IRF3 phosphorylation is stronger in the QKO cells than in WT cells upon poly(I:C) transfection. Interestingly, two genetically independent QKO cells exhibited slightly different kinetics of IRF3 phosphorylation upon poly(I:C) transfection. To test if additional IRF3-dependent genes are also upregulated in the absence of QKI, we assessed mRNA levels of IFN λ 1, IFIT1 and IFIT2 in HuH7 QKO#3 cells. RT-qPCR analysis shows that all of these mRNAs increase in the QKO#3 cells compared with the WT cells. In line with these data, we performed luciferase reporter assays using reporter plasmids containing the IRF3 responsive element in the promoter region; the results show that poly(I:C) triggered more robust IRF3 activation in the QKO#3 cells, suggesting that IRF3 is the key factor that contributes to enhanced IFN induction in the absence of QKI. As ATF2 and cJun are critical transcription factors for optimal IFN β induction [47], we also examined the phosphorylation status of ATF2 and cJun in poly(I:C)-transfected cells. Immunoblotting results showed no dramatic difference in phosphorylation of ATF2 and cJun between WT and the QKO cells. This observation, however, does not exclude the possibility that QKI may regulate other signalling factors. In fact, QKI has been shown to negatively regulate p38 phosphorylation in MAPK signalling [64]. Additionally, elevated p65 phosphorylation in NF κ B pathway was detected in QKI knocked down cells upon LPS stimulation [65]. The functional consequence of these QKI-mediated alterations is the increase of pro-inflammatory cytokine production. As a result, QKI-deficient mice are hyper-responsive to LPS-induced endotoxic shock, parallel with higher levels of TNF- α , IL-6 and IL-1 β in the serum [65]. Collectively, these studies are in line with our finding that QKI inhibits IFN induction.

The three isoforms of QKI play different roles in regulating many biological processes. Although all isoforms share identical amino terminal RNA-binding motifs and presumably bind to similar pools of RNA species via QRE [36], they differ at the carboxyl terminus. This dissimilarity allows these isoforms to regulate the expression level of different pools of RNAs. Consistent with this, RNA-seq analysis reveals that QKI-5 and QKI-6/7 knocked down cells exhibit differential transcriptome profiles [26]. In addition, knock-down of QKI-7, but not QKI-5, was shown to reduce ISG expression in human astrocyte glioma cells [66]. These reports argue that QKI isoforms cooperate and have non-redundant, perhaps partially overlapping, biological functions. In our complementation experiments, expression of QKI-5 alone rescued the phenotype and reduced IRF3 phosphorylation, indicating that QKI-5 is sufficient to repress IRF3 phosphorylation in HuH7 cells. The detailed molecular mechanisms behind this inhibitory effect remain to be elucidated. As spliced variants of IRF3 have been reported to negatively regulate its function [67–69], it would be of interest to test if these splicing events are dependent on QKI-5. An optimal QKI-5 expression level is required to suppress IRF3 phosphorylation (about 80% of WT level). Complemented cells that expressed low QKI-5 level (Q5B2) or high QKI-5 level (Q5B6) failed to rescue the IRF3 phosphorylation phenotype. These results indicate that QKI expression level is a critical parameter for its biological functions. Indeed, QKI expression level is intricately regulated and undergoes dynamic changes during several biological processes. Examples include the following. First, QKI isoform levels are subject to autoregulation [26]. Second, QKI levels can be modulated by microRNAs, and dysregulated alteration may lead to human diseases [64,70]. Third, all QKI isoforms are upregulated during monocyte and myoblast differentiation [25,37]. Fourth, QKI expression level can be impacted by exogenous stimulation, e.g. LPS challenge [65].

QKI plays versatile roles in regulating viral replication. Given that the QKO cells exhibit more robust and stronger IFN response, it is expected that lower infectious viral particle production would be detected in the absence of QKI. This is consistent with a pro-viral role of QKI for Herpes Simplex-1 virus and Zika virus [42,43]. Nonetheless, it is paradoxical with our earlier study, in which QKI knock-down (KD) by siRNA led to increased infectious virion production of a clinical isolate of DENV4 [44]. We reckon that this dual function of QKI in regulating viral replication can be due to the following reasons. First, QKI expression level is key for its biological function. CRISPR-Cas9-mediated KO and siRNA-mediated KD results in different QKI levels in cells. Thus, enhanced IFN response might not be detected in QKI KD cells. Second, viruses harbour different genetic components interacting with host proteins. In particular, the DENV4 clinical isolate we tested before has a QRE in its 3' UTR and it is subject to QKI-3' UTR QRE mediated translational inhibition [44]. Therefore, QKI depletion by siRNA would release this inhibition and increase DENV4 infectious virion production. On the contrary, other viruses that do not contain a QRE in the 3' UTR are likely immune to this QKI-mediated inhibition.

In summary, we demonstrate here a role for QKI in repressing host IFN response via negatively regulating MAVS levels

(Fig. 7). Although higher levels of MAVS are beneficial towards containing viral infection, persistent overexpression of MAVS may lead to IFN-mediated auto-inflammation and auto-immunity. To this end, it would be of great interest to investigate whether QKI plays a role in IFN-dysregulated diseases, which could provide potential opportunities for the development of therapeutic interventions.

Materials and methods

Cell lines and antibodies

HuH7 and A549 cells were maintained in Dulbecco's Modified Eagle Medium (DMEM, Gibco) supplemented with 10% foetal bovine serum (FBS), 100U/mL penicillin and 100µg/mL streptomycin (Pen Strep, Gibco), and 10mM HEPES (Gibco) in a 37°C humidified incubator with 5% CO₂. Tetracycline-inducible cell lines were generated using the Flp-In T-REx system (Thermo Fisher Scientific) according to manufacturer's protocol. After introduction of transgenes, HEK-293 Flp-In T-REx cells were grown in medium with 100µg/mL of hygromycin B and 15 µg/mL of blasticidin. The following primary antibodies were utilized during Western blotting: mouse pan-QKI antibody (clone N147/6; UC Davis/NIH NeuroMab Facility), rabbit QKI-5 antibody (A300-183A; Bethyl Laboratories), mouse pan-actin antibody (MAS-11,869; Thermo Fisher Scientific), rabbit PKR antibody (32,052; Abcam), rabbit IFITM2 antibody (13,530; Cell Signalling), rabbit phosphorylated IRF3 antibody (4947 and 29047; Cell Signalling), rabbit IRF3 antibody (11904; Cell Signalling), rabbit MAVS antibody (3993; Cell Signalling), mouse RIG-I antibody (AG-20B-0009; Adipogen), mouse FLAG antibody (F3165; Sigma), rabbit ISG15 antibody (2743; Cell Signalling), rabbit phosphorylated ATF2 antibody (9225; Cell Signalling), rabbit phosphorylated cJun antibody (3270; Cell Signalling), and rabbit MDA5 antibody (5321; Cell Signalling).

Poly(I:C) transfection

HuH7 cells were seeded at 7.5×10^4 cells per well in 24-well plates the day before stimulation. Cells were transfected with poly(I:C) (HMW; InvivoGen) using Lipofectamine RNAiMAX reagent (Invitrogen) following manufacturer's protocol.

Plasmid construction

QKI-5 gene was amplified using FLAG-QKI-5 F and FLAG-QKI-5 R primers (Supplementary Table S3). The PCR product was digested with the restriction enzymes BamHI and NotI and then ligated into pcDNA3. MAVS gene was amplified from the cDNA (RC208175; Origene) using MAVS F and MAVS R primers. The PCR product was digested with restriction enzymes KpnI and XhoI and then ligated into pcDNA3. For constructing psiCHECK2 P31x3 plasmid, primers P31x3 F and P31x3 R were first mixed at equal molar concentration, and DNA polymerase was added for extension: 95°C for 5min, 55°C for 30s, and 72°C for 10mins. The resultant product was resolved by agarose gel electrophoresis. A band of 193bp size was isolated and purified. This product was

digested with restriction enzymes BglII and NheI and then ligated into psiCHECK2 (Promega). Primer sequences are listed in Supplementary Table S3.

Generation of knockout cell lines and genotyping analysis

Knockout of targeted genes in HuH7 and A549 cells was achieved by using the CRISPR/Cas9 system as previously described [71]. In brief, guide RNA (gRNA) sequence targeting QKI was designed using the CRISPR design tool (<http://crispr.mit.edu>) and both QKI and MAVS [72] targeting gRNA sequences used are listed in Supplementary Table S1. Oligos corresponding to the gRNA sequences were synthesized and cloned into the pSpCas9(BB)-2A-GFP (PX458) (Addgene 48,138). HuH7 and A549 cells were transfected with PX458 plasmids using Lipofectamine 2000 (Thermo Fisher Scientific). After 48h, GFP positive cells were sorted using FACSaria II (BD Biosciences). Sorted cells were directly collected and plated as single clonal cells on a 96-well plate. Alternatively, sorted cells were collected as polyclonal cells first and then limiting dilution in a 96-well plate was performed to isolate single clonal cells. The knockout was confirmed by Western blotting and genotyping analysis. For genotyping QKI KO cells, genomic DNA was isolated using DNeasy Blood & Tissue Kit (Qiagen). Regions spanning the QKI gRNA targeting site were amplified using primers QKI KO scr F and QKI KO scr R (Supplementary Table S3). The PCR product were digested with restriction enzymes BamHI and XbaI and then ligated into pcDNA3. Five clones were sent for sequencing. For genotyping MAVS KO cells, genomic DNA was isolated as mentioned above. Primers MAVS KO scr F and MAVS KO scr R (Supplementary Table S3) were used to amplify regions spanning MAVS gRNA targeting site. The resultant PCR products were ligated into pMiniT 2.0 vector using PCR cloning kit (NEB) for sequencing.

Generation of complemented stable cell lines

HuH7 QKO#3 cells were transfected with 1.5µg plasmids expressing FLAG-tagged QKI-5 using Lipofectamine 2000 (Thermo Fisher Scientific). Approximately 24h after transfection, 1000µg/mL Geneticin (Thermo Fisher Scientific) was used to select for cells stably expressing FLAG-tagged QKI-5 (Q5B). To obtain clonal complemented cells (Q5B2, Q5B4, and Q5B6), limiting serial dilution in a 96-well plate using Q5B polyclonal cells was performed.

Western blotting and densitometry analysis

After treatment, cells were rinsed once with PBS and then were lysed in RIPA buffer (Cell Signalling Technology). For detection of phosphorylated proteins, phosphatase inhibitor cocktail (PhosSTOP; Roche) was added at 1 tablet per 10mL of RIPA buffer. Proteins were separated under denaturing conditions on 4–15% polyacrylamide gels (Bio-Rad). After samples were transferred to polyvinylidene difluoride membranes (PVDF, Bio-Rad), blots were blocked in PBST (0.5% Tween-20) with 5% blotting grade blocker (170–6404; Bio-Rad) or TBST (Tris-buffered saline

with 0.1% Tween-20) with 5% BSA (A7906–100G; Sigma Aldrich) for detection of phosphorylated proteins. Blots were then washed and incubated with primary antibodies overnight at 4°C. Goat anti-mouse HRP (115-035-003; Jackson ImmunoResearch) and goat anti-rabbit HRP (111-035-003; Jackson ImmunoResearch) were used to visualize blots on a chemiluminescence imaging system (Bio-Rad). Densitometry analysis was performed using ImageJ [73].

RNA isolation and real time quantitative PCR (RT-qPCR) analysis

HuH7 cells were seeded at 7.5×10^4 cells per well in 24-well plates the day before stimulation. Cells were transfected with 2 µg poly(I:C) for 4h, unless otherwise indicated, to evaluate RNA levels of *IFNβ*, *IFNλ1*, *IFIT1*, *IFIT2*, *PKR*, *MAVS*, *HPRT1* and *SDHA*. After extracting RNA via the EZNA Total RNA Kit I (OMEGA bio-tek), RapidOut DNA removal kit (Thermo Fisher Scientific) was used to remove genomic DNA. RNA concentrations were measured using NanoDrop spectrophotometer. These samples were then reverse transcribed with the iScript cDNA synthesis kit (Bio-Rad), and RT-qPCR was performed using SensiFAST SYBR No-ROX reagent (BioLine) or SsoAdvanced Universal SYBR Green Supermix (BioRad) according to manufacturer's protocol. RT-qPCR cycling conditions are: 98°C for 1 minutes, [98°C 10 seconds, 60°C 25 seconds] (40 cycles). Relative RNA levels of indicated genes were normalized to the geometric mean of *SDHA* and *HPRT1*, and are expressed relative to the control in each experiment. Primer sequences are listed in the Supplementary Table S3.

RNA immunoprecipitation (RIP)

Flp-In T-REx HEK-293 cells expressing FLAG-tagged QKI-5 were seeded at 1.5×10^6 cells in 10cm dishes. One day post seeding, cells were treated with 5 µg/mL tetracycline to induce protein expression. At 18 hours after tetracycline induction, cells were harvested, pelleted, and lysed in a buffer volume roughly equivalent to the cell pellet volume of RIP lysis buffer (200mM KCl, 20mM HEPES pH7.2, 2% *N*-dodecyl-β-D-maltoside, 1% Igepal CA-360, 100U/mL Murine RNase inhibitor [NEB]). Subsequent lysates were cleared by centrifugation, and protein was normalized across samples to about 200 µg per RIP reaction. To prepare RIP assay beads, Dynabeads protein G (Invitrogen) were blocked with BSA on the day before cell harvest and then incubated with 5 µg of mouse IgG control antibody or 5 µg FLAG antibody with head-to-tail rotation at 4°C overnight. Antibody-coupled beads were washed three times with RIP assay buffer (50mM Tris HCl pH 7.5, 150mM NaCl, 1mM MgCl₂, and 0.05% Igepal CA-360) and subsequently incubated with the prepared lysates on rotation at 4°C for 1 hour. Complexes were washed four times in RIP assay buffer, and immunoprecipitated protein and RNA (extracted by RNazol® RT (Molecular Research Centre)) were analysed by immunoblotting and RT-qPCR, respectively. Primer sequences are listed in the Supplementary Table S3.

Reporter assay

HuH7 cells were seeded at 7.5×10^4 cells per well in 24-well plates the day before transfection. Cells were co-transfected with 150ng IFNβ Firefly luciferase (F Luc) reporter plasmids and 15ng *Renilla* luciferase (R Luc) plasmids using Lipofectamine 3000 (Thermo Fisher Scientific). On the following day, cells were stimulated via either poly(I:C) transfection or Sendai virus (SeV) infection. At 8h post poly(I:C) transfection or 16h post SeV infection, cells were lysed and luciferase activity was analysed using the Dual Luciferase Reporter Assay kit (Promega) on a Spark microplate reader (Tecan). Regarding ectopic expression experiments, 50ng pcDNA3 vector or 50ng plasmids encoding RIG-I were co-transfected with 200ng IFNβ F Luc and 50ng R Luc reporter plasmids into cells. Approximately 24h after transfection, cells were transfected with poly(I:C) for 8h and lysates were analysed as mentioned above. For psiCHECK2 plasmid reporter experiments, 10ng psiCHECK2 vector (Promega) or 250ng psiCHECK2 P31X3 plasmids were transfected into cells using Lipofectamine 3000. Approximately 24h after transfection, cells were transfected with poly(I:C) for 8h and then lysates were analysed as mentioned above.

Viruses and infections

Sendai virus (Cantell Strain; Charles River) infection of HuH7 cells was performed at 25, 50 or 100HA U/mL in serum-free media (DMEM containing 100U/mL penicillin, 100 µg/mL streptomycin and 10mM HEPES) for 1h. The inoculum was then substituted with reduced-serum media (DMEM containing 2% FBS, 100U/mL penicillin, 100 µg/mL streptomycin and 10mM HEPES). At 16h post infection, cells were washed with PBS and processed for reporter assay.

Acknowledgments

We thank Dr. Pradeep Bist at Duke-NUS Medical School, Singapore, for providing reagents for this study. We thank Drs. Shang Li and Muhammad Khairul Ramlee for their advice in creating CRISPR KO cell lines. We are grateful to Dr. Manoj Krishnan for reagents and critical discussion for this project. We also thank all members of the Pompon/Garcia-Blanco laboratory, Duke-NUS Medical School, and colleagues from Bradrick/Garcia-Blanco laboratory, University of Texas Medical Branch, for their input and suggestions during the course of this work.

Disclosure statement

No potential conflicts of interest were disclosed.

Funding

This research was supported by the National Research Foundation Singapore under its Cooperative Basic Research Grant (NMRC/CBRG/0074/2014); by the Singapore Ministry of Health's National Medical Research Council under its Young Individual Research Grant (NMRC/OFYIRG/0054/2017), and under its NMRC Zika Response Research Fund (NMRC/ZRRF/0007/2017) and by the Duke-NUS Medical School Signature Research Programme funded by the Agency for Science, Technology and Research (A*STAR), Singapore, and the Ministry of Health, Singapore.

ORCID

Kuo-Chieh Liao  <http://orcid.org/0000-0002-8766-4824>
 W. Samuel Fagg  <http://orcid.org/0000-0003-2909-1666>
 Julien Pompon  <http://orcid.org/0000-0003-1110-9039>
 Mariano A. Garcia-Blanco  <http://orcid.org/0000-0001-8538-1997>

References

- [1] Trinchieri G. Type I interferon: friend or foe? *J Exp Med.* 2010;207:2053–2063.
- [2] Uematsu S, Akira S. Toll-like receptors and type I interferons. *J Biol Chem.* 2007;282:15319–15323.
- [3] Chow KT, Gale M Jr., Loo YM. RIG-I and other RNA sensors in antiviral immunity. *Annu Rev Immunol.* 2018;36:667–694.
- [4] Loo YM, Fornek J, Crochet N, et al. Distinct RIG-I and MDA5 signaling by RNA viruses in innate immunity. *J Virol.* 2008;82:335–345.
- [5] Kato H, Takeuchi O, Mikamo-Satoh E, et al. Length-dependent recognition of double-stranded ribonucleic acids by retinoic acid-inducible gene-I and melanoma differentiation-associated gene 5. *J Exp Med.* 2008;205:1601–1610.
- [6] Kato H, Takeuchi O, Sato S, et al. Differential roles of MDA5 and RIG-I helicases in the recognition of RNA viruses. *Nature.* 2006;441:101–105.
- [7] Meylan E, Curran J, Hofmann K, et al. Cardif is an adaptor protein in the RIG-I antiviral pathway and is targeted by hepatitis C virus. *Nature.* 2005;437:1167–1172.
- [8] Seth RB, Sun L, Ea CK, et al. Identification and characterization of MAVS, a mitochondrial antiviral signaling protein that activates NF-kappaB and IRF 3. *Cell.* 2005;122:669–682.
- [9] Xu LG, Wang YY, Han KJ, et al. VISA is an adapter protein required for virus-triggered IFN-beta signaling. *Mol Cell.* 2005;19:727–740.
- [10] Kawai T, Takahashi K, Sato S, et al. IPS-1, an adaptor triggering RIG-I- and Mda5-mediated type I interferon induction. *Nat Immunol.* 2005;6:981–988.
- [11] Honda K, Takaoka A, Taniguchi T. Type I interferon gene induction by the interferon regulatory factor family of transcription factors. *Immunity.* 2006;25:349–360.
- [12] Schneider WM, Chevillotte MD, Rice CM. Interferon-stimulated genes: a complex web of host defenses. *Annu Rev Immunol.* 2014;32:513–545.
- [13] Ye C, Yu Z, Xiong Y, et al. STAU1 binds to IBDV genomic double-stranded RNA and promotes viral replication via attenuation of MDA5-dependent beta interferon induction. *Faseb J.* 2019;33:286–300.
- [14] Haque N, Ouda R, Chen C, et al. ZFR coordinates crosstalk between RNA decay and transcription in innate immunity. *Nat Commun.* 2018;9:1145.
- [15] Herdy B, Karonitsch T, Vladimer GI, et al. The RNA-binding protein HuR/ELAVL1 regulates IFN-beta mRNA abundance and the type I IFN response. *Eur J Immunol.* 2015;45:1500–1511.
- [16] Bidet K, Dadlani D, Garcia-Blanco MA. G3BP1, G3BP2 and CAPRIN1 are required for translation of interferon stimulated mRNAs and are targeted by a dengue virus non-coding RNA. *PLoS Pathog.* 2014;10:e1004242.
- [17] Lumb JH, Li Q, Popov LM, et al. DDX6 represses aberrant activation of interferon-stimulated genes. *Cell Rep.* 2017;20:819–831.
- [18] Dixit U, Pandey AK, Mishra P, et al. Staufen1 promotes HCV replication by inhibiting protein kinase R and transporting viral RNA to the site of translation and replication in the cells. *Nucleic Acids Res.* 2016;44:5271–5287.
- [19] Schoggins JW, Wilson SJ, Panis M, et al. A diverse range of gene products are effectors of the type I interferon antiviral response. *Nature.* 2011;472:481–485.
- [20] Ebersole TA, Chen Q, Justice MJ, et al. The quaking gene product necessary in embryogenesis and myelination combines features of RNA binding and signal transduction proteins. *Nat Genet.* 1996;12:260–265.
- [21] Kondo T, Furuta T, Mitsunaga K, et al. Genomic organization and expression analysis of the mouse qkI locus. *Mamm Genome.* 1999;10:662–669.
- [22] Wu J, Zhou L, Tonissen K, et al. The quaking I-5 protein (QKI-5) has a novel nuclear localization signal and shuttles between the nucleus and the cytoplasm. *J Biol Chem.* 1999;274:29202–29210.
- [23] Pilotte J, Larocque D, Richard S. Nuclear translocation controlled by alternatively spliced isoforms inactivates the QUAKING apoptotic inducer. *Genes Dev.* 2001;15:845–858.
- [24] Darbelli L, Richard S. Emerging functions of the Quaking RNA-binding proteins and link to human diseases. *Wiley Int Rev RNA.* 2016;7:399–412.
- [25] Hall MP, Nagel RJ, Fagg WS, et al. Quaking and PTB control overlapping splicing regulatory networks during muscle cell differentiation. *RNA.* 2013;19:627–638.
- [26] Fagg WS, Liu N, Fair JH, et al. Autogenous cross-regulation of Quaking mRNA processing and translation balances Quaking functions in splicing and translation. *Genes Dev.* 2017;31:1894–1909.
- [27] Hayakawa-Yano Y, Suyama S, Nogami M, et al. An RNA-binding protein, Qki5, regulates embryonic neural stem cells through pre-mRNA processing in cell adhesion signaling. *Genes Dev.* 2017;31:1910–1925.
- [28] Li J, Choi PS, Chaffer CL, et al. An alternative splicing switch in FLNB promotes the mesenchymal cell state in human breast cancer. *Elife.* 2018;7. pii: e37184.
- [29] Conn SJ, Pillman KA, Toubia J, et al. The RNA binding protein quaking regulates formation of circRNAs. *Cell.* 2015;160:1125–1134.
- [30] Gupta SK, Garg A, Bar C, et al. Quaking inhibits doxorubicin-mediated cardiotoxicity through regulation of cardiac circular RNA expression. *Circ Res.* 2018;122:246–254.
- [31] Larocque D, Galarneau A, Liu HN, et al. Protection of p27(Kip1) mRNA by quaking RNA binding proteins promotes oligodendrocyte differentiation. *Nat Neurosci.* 2005;8:27–33.
- [32] Thangaraj MP, Furber KL, Gan JK, et al. RNA-binding protein Quaking stabilizes Sirt2 mRNA during oligodendroglial differentiation. *J Biol Chem.* 2017;292:5166–5182.
- [33] Chen AJ, Paik JH, Zhang H, et al. STAR RNA-binding protein Quaking suppresses cancer via stabilization of specific miRNA. *Genes Dev.* 2012;26:1459–1472.
- [34] Wang Y, Vogel G, Yu Z, et al. The QKI-5 and QKI-6 RNA binding proteins regulate the expression of microRNA 7 in glial cells. *Mol Cell Biol.* 2013;33:1233–1243.
- [35] Wang F, Song W, Zhao H, et al. The RNA-binding protein QKI5 regulates primary miR-124-1 processing via a distal RNA motif during erythropoiesis. *Cell Res.* 2017;27:416–439.
- [36] Galarneau A, Richard S. Target RNA motif and target mRNAs of the Quaking STAR protein. *Nat Struct Mol Biol.* 2005;12:691–698.
- [37] de Bruin RG, Shiue L, Prins J, et al. Quaking promotes monocyte differentiation into pro-atherogenic macrophages by controlling pre-mRNA splicing and gene expression. *Nat Commun.* 2016;7:10846.
- [38] Yang G, Fu H, Zhang J, et al. RNA-binding protein quaking, a critical regulator of colon epithelial differentiation and a suppressor of colon cancer. *Gastroenterology.* 2010;138(231–40):e1–5.
- [39] Zong FY, Fu X, Wei WJ, et al. The RNA-binding protein QKI suppresses cancer-associated aberrant splicing. *PLoS Genet.* 2014;10:e1004289.
- [40] de Miguel FJ, Pajares MJ, Martinez-Terroba E, et al. A large-scale analysis of alternative splicing reveals a key role of QKI in lung cancer. *Mol Oncol.* 2016;10:1437–1449.
- [41] Li F, Yi P, Pi J, et al. QKI5-mediated alternative splicing of the histone variant macroH2A1 regulates gastric carcinogenesis. *Oncotarget.* 2016;7:32821–32834.
- [42] Sanchez-Quiles V, Mora MI, Segura V, et al. HSV-1 Cgal+ infection promotes quaking RNA binding protein production and induces nuclear-cytoplasmic shuttling of quaking I-5 isoform in human hepatoma cells. *Mol Cell Proteomics.* 2011;10:M111 009126.
- [43] Ramanathan M, Majzoub K, Rao DS, et al. RNA-protein interaction detection in living cells. *Nat Methods.* 2018;15(3):207–212

- [44] Liao KC, Chuo V, Ng WC, et al. Identification and characterization of host proteins bound to dengue virus 3' UTR reveal an antiviral role for quaking proteins. *RNA*. 2018;24:803–814.
- [45] Li K, Chen Z, Kato N, et al. Distinct poly(I-C) and virus-activated signaling pathways leading to interferon-beta production in hepatocytes. *J Biol Chem*. 2005;280:16739–16747.
- [46] Yoneyama M, Kikuchi M, Matsumoto K, et al. Shared and unique functions of the DExD/H-box helicases RIG-I, MDA5, and LGP2 in antiviral innate immunity. *J Immunol*. 2005;175:2851–2858.
- [47] Kim TK, Maniatis T. The mechanism of transcriptional synergy of an in vitro assembled interferon-beta enhanceosome. *Mol Cell*. 1997;1:119–129.
- [48] Grandvaux N, Servant MJ, tenOever B, et al. Transcriptional profiling of interferon regulatory factor 3 target genes: direct involvement in the regulation of interferon-stimulated genes. *J Virol*. 2002;76:5532–5539.
- [49] Osterlund PI, Pietila TE, Veckman V, et al. IFN regulatory factor family members differentially regulate the expression of type III IFN (IFN-lambda) genes. *J Immunol*. 2007;179:3434–3442.
- [50] Lee HC, Narayanan S, Park SJ, et al. Transcriptional regulation of IFN-lambda genes in hepatitis C virus-infected hepatocytes via IRF-3, IRF-7, NF-kappaB complex. *J Biol Chem*. 2014;289:5310–5319.
- [51] Wathelet MG, Lin CH, Parekh BS, et al. Virus infection induces the assembly of coordinately activated transcription factors on the IFN-beta enhancer in vivo. *Mol Cell*. 1998;1:507–518.
- [52] Xu L, Peng L, Gu T, et al. The 3'UTR of human MAVS mRNA contains multiple regulatory elements for the control of protein expression and subcellular localization. *Biochim Biophys Acta Gene Regul Mech*. 2019;1862:47–57.
- [53] Liu B, Gao C. Regulation of MAVS activation through post-translational modifications. *Curr Opin Immunol*. 2018;50:75–81.
- [54] Peisley A, Wu B, Yao H, et al. RIG-I forms signaling-competent filaments in an ATP-dependent, ubiquitin-independent manner. *Mol Cell*. 2013;51:573–583.
- [55] Saito T, Hirai R, Loo YM, et al. Regulation of innate antiviral defenses through a shared repressor domain in RIG-I and LGP2. *Proc Natl Acad Sci U S A*. 2007;104:582–587.
- [56] Ogilvie RL, Sternjohn JR, Rattenbacher B, et al. Tristetraprolin mediates interferon-gamma mRNA decay. *J Biol Chem*. 2009;284:11216–11223.
- [57] Schmidtko L, Schrick K, Saurin S, et al. The KH-type splicing regulatory protein (KSRP) regulates type III interferon expression post-transcriptionally. *Biochem J*. 2019;476:333–352.
- [58] Witteveldt J, Ivens A, Macias S. Inhibition of microprocessor function during the activation of the type I interferon response. *Cell Rep*. 2018;23:3275–3285.
- [59] Suthar MS, Ma DY, Thomas S, et al. IPS-1 is essential for the control of West Nile virus infection and immunity. *PLoS Pathog*. 2010;6:e1000757.
- [60] Rivera-Serrano EE, DeAngelis N, Sherry B. Spontaneous activation of a MAVS-dependent antiviral signaling pathway determines high basal interferon-beta expression in cardiac myocytes. *J Mol Cell Cardiol*. 2017;111:102–113.
- [61] Wan S, Ashraf U, Ye J, et al. MicroRNA-22 negatively regulates poly(I:C)-triggered type I interferon and inflammatory cytokine production via targeting mitochondrial antiviral signaling protein (MAVS). *Oncotarget*. 2016;7:76667–76683.
- [62] Hsu AC, Dua K, Starkey MR, et al. MicroRNA-125a and -b inhibit A20 and MAVS to promote inflammation and impair antiviral response in COPD. *JCI Insight*. 2017;2:e90443.
- [63] Ebert MS, Sharp PA. Roles for microRNAs in conferring robustness to biological processes. *Cell*. 2012;149:515–524.
- [64] Tili E, Chiabai M, Palmieri D, et al. Quaking and miR-155 interactions in inflammation and leukemogenesis. *Oncotarget*. 2015;6:24599–24610.
- [65] Wang L, Zhai DS, Ruan BJ, et al. Quaking deficiency amplifies inflammation in experimental endotoxemia via the aryl hydrocarbon receptor/signal transducer and activator of transcription 1-NF-kappaB pathway. *Front Immunol*. 2017;8:1754.
- [66] Jiang L, Saetre P, Radomska KJ, et al. QKI-7 regulates expression of interferon-related genes in human astrocyte glioma cells. *PLoS One*. 2010;5. pii: e13079.
- [67] Karpova AY, Ronco LV, Howley PM. Functional characterization of interferon regulatory factor 3a (IRF-3a), an alternative splice isoform of IRF-3. *Mol Cell Biol*. 2001;21:4169–4176.
- [68] Marozin S, Altomonte J, Stadler F, et al. Inhibition of the IFN-beta response in hepatocellular carcinoma by alternative spliced isoform of IFN regulatory factor-3. *Mol Ther*. 2008;16:1789–1797.
- [69] Li C, Ma L, Chen X. Interferon regulatory factor 3-CL, an isoform of IRF3, antagonizes activity of IRF3. *Cell Mol Immunol*. 2011;8:67–74.
- [70] Pillman KA, Phillips CA, Roslan S, et al. miR-200/375 control epithelial plasticity-associated alternative splicing by repressing the RNA-binding protein Quaking. *Embo J*. 2018;37(13). pii: e99016.
- [71] Ran FA, Hsu PD, Wright J, et al. Genome engineering using the CRISPR-Cas9 system. *Nat Protoc*. 2013;8:2281–2308.
- [72] Bender S, Reuter A, Eberle F, et al. Activation of type I and III interferon response by mitochondrial and peroxisomal MAVS and inhibition by hepatitis C virus. *PLoS Pathog*. 2015;11:e1005264.
- [73] Schneider CA, Rasband WS, Eliceiri KW. NIH image to imageJ: 25 years of image analysis. *Nat Methods*. 2012;9:671–675.